Misfolded α-synuclein causes hyperactive respiration without functional deficit in live neuronal cells

Ugalde C.L[1,2,3,4], Annesley S.J[5], Mroczek K[5], Lawson V.A[2], Fisher P.R[5], Finkelstein D.I[3], Hill, A.F[1,4*]

[1] La Trobe Institute for Molecular Science, La Trobe University, Bundoora, Victoria, Australia 3082;

[2] Department of Microbiology and Immunology, University of Melbourne, Parkville, Victoria, Australia 3052;

[3] Howard Florey Institute of Neuroscience and Mental Health, Parkville, Victoria, Australia 3052;

[4] Department of Biochemistry and Molecular Biology, University of Melbourne, Parkville, Victoria, Australia 3052

[5] Department of Physiology, Anatomy and Microbiology, La Trobe University, Bundoora, Victoria, Australia 3082

[*]To whom correspondence should be addressed: Andrew F Hill: La Trobe Institute for Molecular Science, La Trobe University, Bundoora, VIC 3086, Australia. andrew.hill@latrobe.edu.au; Tel. +61 3 9479-1224

Key words: α-synuclein, synucleinopathy, Parkinson's disease, mitochondria, cardiolipin, PMCA

Summary statement: Misfolded α-synuclein that was produced using the Protein Misfolding Cyclic Amplification (PMCA) assay was found to associate with cardiolipin and cause hyperactive respiration in neuronal cells.

Abstract

The misfolding and aggregation of the largely disordered protein, α-synuclein (αsyn), is a central pathogenic event that occurs in the synucleinopathies; a group of neurodegenerative disorders that includes Parkinson's disease. While there is a clear link between protein misfolding and neuronal vulnerability, the precise pathogenic mechanisms employed by disease-associated αsyn are unresolved. Here, we studied the pathogenicity of a heterogeneous population of misfolded αsyn produced using the Protein Misfolding Cyclic Amplification (PMCA) assay. To do this, previous published methods were adapted to allow PMCA-induced protein fibrillization to occur under non-toxic conditions. Insight into potential intracellular targets of misfolded αsyn was obtained using an unbiased lipid screen of 15 biologically relevant lipids that identified cardiolipin (CA) as a binding partner for PMCA-generated misfolded αsyn. To investigate if this interaction can impact the properties of αsyn misfolding, protein fibrillization was carried out in the presence of the lipid. We show CA both accelerates the rate of αsyn fibrillization and produces species that harbour enhanced resistance to proteolysis. Because CA is

virtually exclusively expressed in the inner mitochondrial membrane, we then assessed the ability of these misfolded species to alter mitochondrial respiration in live non-transgenic neuronal cells. Extensive analysis revealed misfolded αsyn causes hyperactive mitochondrial respiration without causing any functional deficit. This data gives strong support for the mitochondrion as a target for misfolded αsyn and reveals persistent, hyperactive respiration as a potential up-stream pathogenic event associated with the synucleinopathies.

Introduction

Parkinson's disease (PD) is a slowly progressing movement disorder clinically defined by the appearance of bradykinesia, rigidity or tremor. Pathological features of PD are the appearance of Lewy Bodies, which are intracellular protein deposits predominately composed of misfolded α-synuclein (αsyn), and neuronal loss. PD is one of a group of neurodegenerative conditions called synucleinopathies that have in common the aggregation of misfolded αsyn. The profiles of neuronal vulnerability and protein deposition within neurons and glial cells vary amongst the conditions (Surmeier et al., 2017, Galvin et al., 2001) and PD is associated with the progressive loss of dopaminergic neurons in the substania nigra pars compacta.

Largely an unstructured protein that is localized to the synapse under normal physiological conditions, the misfolding of αsyn is strongly linked to the development of disease. This is evidenced by the finding that various point mutations in the gene encoding αsyn, *SNCA*, causes early onset familial disease (Polymeropoulos et al., 1997, Kruger et al., 1998, Zarranz et al., 2004, Appel-Cresswell et al., 2013, Proukakis et al., 2013, Lesage et al., 2013) as do gene duplications (Chartier-Harlin et al., 2004) and triplications (Singleton et al., 2003). Likewise, there is also now a large body of data showing the ability of αsyn to adopt pathogenic properties upon misfolding (reviewed in: (Ugalde et al., 2016)).

Despite the numerous data describing the pathogenicity of misfolded αsyn, the precise molecular mechanisms αsyn employs that contribute to the pathogenesis of the synucleinopathies is currently unclear. A consideration to studying these disorders is the complex nature of αsyn misfolding, which as an amyloid forming protein, can adopt numerous misfolded conformations. Precursors to the mature fibrils abundant in LBs, small soluble oligomers and protofibrils also present in the brain in PD (Garcia-Esparcia et al., 2015, Sharon et al., 2003, Tofaris et al., 2003) and critically, oligomers are considered to be the most toxic conformation (reviewed in (Ugalde et al., 2016)). The process of αsyn fibril-formation sees these highly dynamic species exist as part of a heterogeneous mix of various sized conformations that maintain a state of equilibrium and through interspecies interactions, can both expand and contract to higher or lower ordered structures (Cremades et al., 2012, Roberts and Brown, 2015).

Many studies examining the properties of pathogenic αsyn induce misfolding in bacterially-expressed recombinant protein to produce a homogenous population of a defined misfolded structure. While these common techniques of fibrillization are useful to attribute pathogenic properties to a specific conformation, they are not reflective of the numerous conformations of pathogenic αsyn that exist *in vivo*. A novel fibrillization technique that may alleviate these issues is the Protein Misfolding Cyclic Amplification (PMCA), which is an assay shown capable of producing various sized misfolded forms of αsyn (Herva et al., 2014). Current studies on the pathogenicity of species formed via PMCA are limited to low concentrations of dilute protein due to a high concentration of detergent in the conversion buffer. As such, we sought to study the properties of PMCA-generated αsyn by adapting published methods to produce misfolded species under non-toxic conditions and extensively characterizing formed species. Next, to gain insight into the pathogenic properties of misfolded αsyn, an unbiased lipid screen of 15 biologically relevant lipids was performed. We show that PMCA-generated αsyn selectively associates with cardiolipin (CA), and further assessment reveals this lipid can both accelerate fibrillization and modify the biochemical properties of αsyn species formed by enhancing their resistance to proteolysis. Given that CA is a lipid almost exclusively expressed in the inner mitochondrial membrane (IMM), we then sought to determine if this interaction has relevance to cellular functioning by assessing the ability of PMCA-generated αsyn to modulate mitochondrial respiration in live non-transgenic neuronal cells. Comprehensive analysis using the Seahorse XF Analyzer showed misfolded αsyn causes hyperactive mitochondrial respiration without causing dysfunctional activity at any complex. This also occurred independently of upstream metabolic changes in glycolysis. This rigorous data in cells with normal endogenous protein confirms the mitochondrion is a target for misfolded αsyn and suggests hyperactive respiration may be an early, up-stream pathogenic process neuronal cells experience in the synucleinopathy disorders.

Results

PMCA can produce misfolded αsyn species in prion conversion buffer (PCB)

Generating misfolded αsyn species using PMCA was first developed following the protocol outlined by Herva et al. (Herva et al., 2014) (Figure 1). The PMCA assay was originally developed to study the generation of the proteinaceous and transmissible neurodegenerative agents, prions (Saborio et al., 2001), and because the buffer used by Herva et al. to dissolve αsyn is routinely used as the conversion buffer for prion PMCA reactions, it is hereafter referred to as the prion conversion buffer (PCB). The extent of fibrillization of αsyn in PCB following exposure to PMCA for 24 h was assessed using western immunoblot, transmission electron microscopy (TEM) and thioflavin T (ThT) fluorescence. Here, western immunoblot was employed to identify small conformations of misfolded αsyn that may be resolved by SDS-PAGE and showed samples subjected to PMCA contained a range of various

sized species, with monomeric protein observed at 14 kDa and dimer, trimer and tetramer oligomers identified by their increase in molecular weight by intervals of the weight of the monomer (Figure 1A). Species greater than a tetramer, separated by the size of one monomeric unit were identified all the way up to the high molecular weight range of the gel. In comparison, a non-PMCA sample stored at -80ºC during the PMCA process was almost entirely composed of monomeric protein (Figure 1A). TEM was next used to confirm the presence of large mature αsyn fibrils. Consistent with the TEM images reported by Herva et al. (Herva et al., 2014), PMCA generated αsyn fibrils were found to be rod-like in structure. No aggregates were observed in the -80ºC sample (Figure 1B). The compound ThT exhibits fluorescence upon binding to β-sheet structures (Vassar and Culling, 1959, Biancalana and Koide, 2010), and hence is universally used to detect amyloid. Upon exposure to 24 h PMCA, αsyn adopted strong ThT reactivity, while the monomeric -80ºC sample displayed no fluorescent signal (Figure 1C). Collectively these data confirm PMCA is a useful tool to produce a range of various-sized αsyn species.

PMCA-induced misfolding of αsyn can occur under non-toxic conditions

Because the PCB used to reconstitute protein in Figure 1 contains Triton X-100, a limitation to studying the pathogenicity of PMCA-generated αsyn is the inherent toxicity of the buffer. Accordingly, in order to progress to studies on the pathogenicity of PMCA-generated αsyn, it was necessary to isolate these species in a buffer that did not contain detergent. Given the small size and highly dynamic nature of oligomers, buffer exchange or centrifugation were not considered viable options to collect or maintain the integrity of the small, oligomeric species. Instead, the replacement of the conversion buffer, PCB, with a non-toxic analogue was pursued. In order to address this, the extent of PMCA-induced fibrillization of αsyn was assessed following its reconstitution in several buffers assumed to be non-toxic. The following buffers were tested: PBS, PBS+150 mM NaCl (PBSN), TBS and TBS+150 mM NaCl (TBSN). These samples were exposed to 24 h PMCA as per the same conditions detailed in Figure 1 and were compared to an equivalent sample of αsyn dissolved in PCB buffer (αsyn:PCB). Western immunoblot and ThT were used as readouts to compare the extent of αsyn fibrillization in the various buffers (Supplementary Figure 1). The ThT data showed that following PMCA, all buffers were able to produce species that contained ThT-reactive conformations (Supplementary Figure 1A). Resolving samples on SDS-PAGE and immunodetection of αsyn gave further information on the αsyn species produced by the buffers (Supplementary Figure 1B). This assay revealed differences in the efficiency of the buffers to induce fibrillization, with PCB clearly being the most proficient buffer for producing oligomeric species. The degree of fibrillization was variable amongst the non-toxic buffers with PBSN being the most effective non-toxic buffer for αsyn misfolding.

Given that none of the non-toxic buffers were as effective as PCB in facilitating misfolding of αsyn, the protocol was further adapted with the most efficient non-toxic buffer, PBSN (Figure 2). Here, the total process time of 24 h was extended to determine if PBSN may produce comparable misfolded αsyn content to PCB if exposed to PMCA for a longer period of time. To this end, an incremental time-course experiment was performed where αsyn:PBSN was subjected to PMCA for a total process time of: 0, 24, 48 and 72 h. These samples were compared to αsyn:PCB exposed to 24 h PMCA. Western immunoblot analysis revealed the abundance of misfolded species produced in PBSN continues to amplify beyond a 24 h PMCA process time, with time-dependent elevations in misfolded content observed in samples exposed to PMCA for 48 h and 72 h. Following exposure to PMCA for 72 h, the presence of oligomeric species in αsyn:PBSN was comparable to 24 h αsyn:PCB (Figure 2A). Similar to 24 h αsyn:PCB shown in Figure 1A, 72 h αsyn:PBSN was ThT-reactive (Figure 2B). Collectively these studies confirm 72 h is an appropriate PMCA process time to produce misfolded species in PBSN. The species formed by αsyn:PBSN were further characterized by TEM and circular dichroism (CD). Using TEM, the morphology of fibrillar species produced in PBSN after PMCA for 72 h (Figure 2C) was found to be consistent with those produced in PCB (Figure 1B and Herva et al. (Herva et al., 2014)). Likewise, the resulting CD spectra are consistent with the organized rearrangement of αsyn upon misfolding whereby the largely random coil present in monomeric protein shifts to become rich in β-sheet following PMCA (Figure 2D), and confirms the misfolding of αsyn in this system is equivalent to PMCA-induced fibrillization in PCB (Herva et al., 2014).

A necessary component to confirming that PBSN is a suitable buffer to produce misfolded αsyn for this study was to confirm PBSN is non-toxic when applied to cultured cells. To address this, the ability of the buffer alone to cause cell death in neuronal SH-SY5Y cells was measured via the release of lactate dehydrogenase (LDH) into conditioned media. Here, cells were treated with PCB or PBSN such that the total volume of culture media was composed of 0.5, 1, 5 or 10% buffer and LDH measured 24 h later (Figure 2E). Results showed a clear dose-dependent increase in toxicity of PCB, with 10% PCB eliciting a near-100% cell death response for SH-SY5Y cells. In contrast, PBSN showed negligible toxicity at all concentrations tested. The cytotoxicity measured by LDH was confirmed by differential interference contrast (DIC) images of cells exposed to PCB or PBSN (Figure 2F).

In order to test the usefulness of PBSN-based buffers in PD-model systems, LDH assays were also performed using the A4 cell line that are SH-SY5Y cells stably transfected to overexpress wild-type αsyn. Prior to LDH measurements, confirmation of elevated αsyn expression in A4 cells compared to untransfected SH-SY5Y counterparts came from western immunoblot and immunofluorescence (Supplementary Figure 2A-B). Similar to untransfected SH-SY5Y cells, 24 h exposure to PBSN was not toxic to A4 cells, while PCB elicited high levels of cell death. These values were corroborated by DIC images of A4 cells treated with both buffers (Supplementary Figure 2D).

Various transition metals have been shown to accelerate αsyn fibrillization. These include copper (Cu) (Uversky et al., 2001), iron (Fe) (Uversky et al., 2001), cobalt (Co) (Uversky et al., 2001), manganese (Mn) (Uversky et al., 2001) and zinc (Zn) (Munishkina et al., 2008), among others. Critically, Cu and Fe have been shown to not only accelerate fibrillization, but also to produce species that are thinner and more 'network-like' than fibrils produced in their absence (Bharathi et al., 2007). Because of this, the concentration of metals within the PBSN buffer was assessed to determine if these metals might be contributing to misfolding in this system. Inductively coupled plasma-mass spectrometry (ICP-MS) was employed to determine abundances of several common elements. Consistent with using a PBS-based buffer, sodium (Na) and phosphorus (P) were the most abundant metals in the samples containing buffer alone (PBSN) and buffer containing 90 μM αsyn (PBSN+αsyn) (Supplementary Table 1). Several metals shown to modulate αsyn fibrillization were recorded as being at or below the detection limit of the instrument: Mn, Fe, Co, Zn (Supplementary Table 1). Importantly, low values were recorded for both Fe and Cu and hence any contribution to αsyn misfolding by relevant metals is negligible.

Collectively, these experiments confirm PBSN is a suitable buffer to produce αsyn species under non-toxic conditions, which greatly improves the capacity of the PMCA to be used as a tool to study pathogenic properties of misfolded αsyn species. As such, all subsequent experiments using PMCA-generated misfolded αsyn were produced using this optimized method.

PMCA-generated misfolded αsyn selectively associates with cardiolipin

The development of a method to produce misfolded αsyn under non-toxic conditions using PMCA allowed the commencement of the next aim, which was to identify potential pathogenic mechanisms of misfolded αsyn. While numerous mechanisms of how αsyn causes cellular damage have been reported, a common theme unifying several of these mechanisms appears to involve the interaction of misfolded αsyn with lipid species (reviewed in: (Ugalde et al., 2019)). Therefore, to gain insight on potential mechanisms to pursue, the ability of misfolded αsyn to interact with various lipids was assessed using a hydrophobic membrane that had been dotted with 15 long chain (>diC16) highly pure synthetic lipid analogues and a blank control. This membrane was incubated with misfolded (PMCA) or monomeric (-80ºC) αsyn and the degree of protein binding to the lipids assessed via immunoblot using the αsyn-specific antibody MJFR1 and quantified as the percent αsyn binding over the blank control. Results revealed that, compared to the -80ºC sample, PMCA αsyn exhibited a general elevation in both lipid-specific and non-specific binding to the membrane (Figure 3A-C). After normalization to the blank control, misfolded αsyn was found to have no propensity to associate with 11 of the lipids (Figure 3A-B). A few classes showed weak binding potential, with phosphatidylcholine, sphingomyelin and sulfatide having a percent binding of lipid normalized to

blank of 110, 105 and 109, respectively. By far, αsyn exhibited the strongest affinity to cardiolipin (CA), which had an elevation of 142% over the blank control (Figure 3B). Interestingly, the interaction of αsyn with these lipid species was conformation specific, with no reactivity with any lipid observed after incubation with the -80ºC sample (Figure 3C). Given that this sample contains monomeric protein and no ordered aggregates, it can be inferred that the protein interacting with lipids in the PMCA sample are ordered misfolded structures.

The identification of CA as a lipid class with high binding affinity to misfolded αsyn merited further analysis into whether this lipid can modulate αsyn fibrillization. To do this, ThT was employed to study the kinetics of αsyn fibrillization in the presence of the lipid. After reconstitution in methanol (MeOH) and PBSN, CA was added to αsyn:PBSN for a final concentration of 77 µg/mL and 7.7 µg/mL. MeOH/PBSN alone was added to tubes with equivalent protein to serve as a control for the effect of the buffer. The ability of CA to modulate αsyn fibrillization was determined by measuring ThT fluoresence in individual tubes containing CA exposed to PMCA for a total process time of: 0, 6, 8, 10, 12, 24 or 72 h and analysed compared to equivalent CA-free control samples. Here, compared to tubes containing αsyn with MeOH/PBSN (buffer only), the addition of 77 µg/mL CA accelerated αsyn fibrillization which was evidenced by a statistically significant elevation in ThT first identified after 10 h ($p=0.031$) (Figure 3D). This elevation was sustained in all subsequent time-points (12, 24 and 72 h; $p=0.009$, 0.041 and 0.006, respectively). No significant differences were identified between the control group and the lower concentration of CA (7.7 µg/mL CA). Importantly, neither the lipid nor MeOH/PBSN exhibited any florescence signal in the absence of αsyn (Figure 3D).

Having observed the ability of CA to modulate αsyn fibrillization detected using a fluorescent technique, we sought to complement these observations by examining what effect this has on the misfolded protein produced. It has been shown that species formed by PMCA are more resistant to proteolysis (Herva et al., 2014) which may be a useful assay to detect changes in the population of species formed. Accordingly, the effect of CA on the misfolding of αsyn was next assessed by exposing PMCA products to proteinase K (PK) digestion and performing western immunoblot. PMCA of αsyn was performed in reactions containing CA (as per the conditions for Figure 3D) or buffer for 72 h prior to being exposed to 0, 2 or 10 µg/mL PK. These samples were compared to corresponding tubes that did not undergo PMCA (-80ºC). Results showed in the absence of proteolysis or low concentrations of PK (2 µg/mL), no discernible difference in αsyn species could be noted between the treatment groups. However, upon treatment with 10 µg/mL PK, an increase in both high and low molecular weight protein was observed in the PMCA sample containing 77 µg/mL CA, compared to all other groups (Figure 3E). Densitometric analysis revealed, in the PMCA samples digested with 10 µg/mL PK, the total protein abundance in the sample containing 77 µg/mL CA was 1.38 fold higher than its buffer control (MeOH/PBSN) equivalent. This altered expression appeared to be due to changes in PK resistant material in the molecular weight range of 90 – 100 kDa and 15 – 20

kDa. On the western immunoblot in Figure 3E, these regions are identified by red arrows. Given that elevated reactivity was observed in both the high and low molecular weight region, these two populations of PK resistant protein likely reflect the large species that were able to resolve further through the gel following PK digestion and their concomitant cleavage products. Both 2 and 10 µg/mL PK digested all protein in all -80ºC groups indicating neither the CA nor buffer interfered with the activity of PK in this experiment. This assay compliments the findings of Figure 3D and indicates that the acceleration of fibrillization seen is associated with changes to the biochemical properties of formed species in this system.

PMCA-generated misfolded αsyn causes mitochondrial hyperactivity without any functional deficit in naïve SH-SY5Y cells

Within a cell, the expression of CA is almost exclusively localized to the IMM. Hence, the finding that misfolded αsyn binds selectively to CA suggests that the mitochondrion is a target for misfolded αsyn. A major biochemical process driven by mitochondria is oxidative phosphorylation that produces the majority of the cell's energy in the form of adenosine triphosphate (ATP). This respiration occurs via the electron transport chain (ETC) which is a series of reactions that take place within the IMM and involves four complexes (I-IV) that collectively act to shuttle electrons between them. This process releases protons into the intermembrane space (IMS); creating a proton gradient between the IMS and the mitochondrial matrix (MM) that in turn drives the generation of ATP through the large multi-subunit enzyme complex, ATP synthase.

We sought to assess the effect misfolded αsyn has on mitochondrial respiration by measuring respiratory flux rates, which are the rates of electron transfer to molecular oxygen via the electron transport chain. This is performed in live cells following the incremental addition of compounds that selectively inhibit components of oxidative phosphorylation. In this regard, information of the functioning of each of the components of oxidative phosphorylation may be obtained. Unlike standard techniques that quantify products of respiration at a single time-point, the ability to measure flux changes in mitochondria is a powerful way to identify both overt and subtle alterations to respiration.

The ability of misfolded αsyn to alter mitochondrial respiration was measured in naïve SH-SY5Y cells using the Seahorse XFe24 Analyzer. In this system, respiration is measured via changes in oxygen (referred to as oxygen consumption rate; OCR) in the media in wells containing adhered cells. This is performed using a solid-state sensor probe that detects changes in dissolved oxygen in a portion of the media over time, with multiple readings taken to increase the sensitivity of the assay. Baseline oxygen consumption rate (OCR) readings were taken on adhered cells, prior to the sequential addition of the pharmacological chemicals oligomycin, carbonyl cyanide m-chlorophenyl hydrazone (CCCP), rotenone and antimycin A. Respectively, these compounds inhibit ATP-synthase,

permeabilize mitochondrial membranes to protons, inhibit complex I and complex III (in the presence of rotenone this inhibits the flow of electrons from Complex II to oxygen). The data obtained from such measurements allows the following parameters to be measured in a single experiment: basal respiration, ATP synthesis, maximum (max) respiration, Complex I activity, Complex II activity, respiratory control ratio, proton leak, coupling efficiency and non-mitochondrial respiration. A schematic showing a typical respirometry experiment is shown in Figure 4A.

In addition to cells exposed to misfolded αsyn, other treatment groups included cells incubated with monomeric αsyn (-80ºC), buffer alone (PBSN) and cells left untreated (Untreat). Figure 4B is an example CRC experiment performed in the current study. Statistical analysis on independent experimental replicates showed cells exposed to misfolded αsyn had an elevated basal OCR compared to both monomeric and buffer-treated cells (Figure 4C). This significant elevation of OCR in the presence of misfolded αsyn was maintained in individual components of mitochondrial respiration; ATP synthesis, max OCR, Complex I activity and non-mitochondrial respiration (Figure 4D-F, 4H). Importantly, no significant difference was found between -80ºC, PBSN and untreated groups in any readout. While Complex II activity was also elevated upon exposure to misfolded αsyn compared to the control groups, this difference did not reach statistical significance in comparisons between any groups (Figure 4G). However, this observation is not unexpected given the low overall contribution of Complex II to the OCR in this cell line, relative to the accuracy and reproducibility of the assay. To summarize this data, misfolded αsyn causes broad-spectrum elevations to all components of respiration in mitochondria of SH-SY5Y cells. This hyperactivity was specific to misfolded αsyn and was not observed in cells treated with monomeric protein, buffer alone or left untreated. Supplementary Table 2 details all significant values from statistical analysis of cellular respiration data shown in Figure 4.

Further analysis of the OCR values obtained in Figure 4 was performed to determine whether the alterations in respiration identified were associated with concomitant functional deficits. The following functional readouts were calculated: basal (% max OCR), ATP (% basal), max (% basal), Complex I (% max OCR), non-mitochondrial respiration (% max OCR) and spare capacity. No difference was seen in any experimental group (Figure 5), indicating that misfolded αsyn does not affect the function and thus fractional contribution to respiration by any of the individual complexes. Therefore, while misfolded αsyn causes mitochondrial hyperactivity, it does not translate to any kind of observable dysfunction in the mitochondria of SH-SY5Y cells.

Hyperactivity is not a result of altered glycolysis in SH-SY5Y cells exposed to misfolded αsyn

Having identified the capacity of misfolded αsyn to cause hyperactive mitochondrial respiration, we next explored whether other components of cellular respiration were similarly affected. Glycolysis is

an important upstream component to cellular respiration; it produces a small amount of the total ATP synthesized by the cell and critically produces acetyl co-enzyme A, which feeds into the tricarboxylic acid cycle, producing the electron donors $FADH_2$ and NADH that are essential for oxidative phosphorylation. Given the intimate association between glycolysis and oxidative phosphorylation, the glycolytic potential of SH-SY5Y cells was assessed upon exposure to misfolded αsyn, which was measured via the extracellular acidification (ECAR) rate of cells in a glycolytic stress test. Within a cellular environment, ECAR is largely attributed to glycolysis and similar to the fluxes in cellular respiration, the glycolytic potential of cells may be tested by the sequential addition of compounds: glucose, oligomycin, rotenone & antimycin A and 2-deoxy-D glucose. The combination of these compounds, respectively, provide fuel for glycolysis to occur, inhibit ATP synthase, inhibit electron transport and inhibit glycolysis. The inhibition of electron transport by the combined actions of rotenone and antimycin A allows assessment of any contribution to ECAR by respiratory electron transport. In these cells under the assay conditions used, respiratory electron transport made no significant difference to the ECAR (for example, Supplementary Figure 3B). Basic parameters calculated from this included starved ECAR, basal glycolytic ECAR, glycolytic capacity and spare glycolytic capacity. An image depicting a typical experiment measuring glycolytic potential is shown in Supplementary Figure 3A. Glycolytic potential of SH-SY5Y cells was measured upon exposure to PMCA-generated misfolded αsyn (PMCA), monomeric αsyn (-80^{o}C), buffer alone (PBSN) and untreated (Untreat) with the same treatment regime as the CRC experiments. An example experiment is shown in Supplementary Figure 3B and following three independent experiments, no difference was found between any of the experimental groups in all glycolytic parameters (Supplementary Figure 3C-F).

Discussion

The PMCA is an assay shown to be capable of producing a range of various sized misfolded αsyn species (Herva et al., 2014). It was of interest to use this system to study the pathogenicity of misfolded αsyn, however further analysis on the species formed was limited due to a high concentration of detergent in the conversion buffer. Hence this study had two components: 1) to adapt the published protocol of PMCA-induced αsyn misfolding to enable their production to occur under non-toxic conditions and 2) to use this newly reformed system to investigate pathogenic mechanisms of misfolded αsyn. Replication of the original protocol was first achieved, with species produced via PMCA being characterized using a range of readouts (ThT, TEM and western immunoblot). This confirmed the system as a suitable tool to produce misfolded αsyn. The effectiveness of PMCA-induced αsyn misfolding when reconstituted in non-toxic buffers was next tested, and adaption of the protocol performed with the most efficient non-toxic buffer, PBSN. New parameters were determined

to produce comparable misfolded content to the initial buffer, with 72 h being the optimized time to misfold αsyn in PBSN. The ability of PBSN to be well tolerated in both normal, untransfected and transgenic PD-model neuronal cells was the final assessment in the adaptation of the protocol and allowed further studies into the cellular targets of misfolded αsyn.

The major finding of this study was that PMCA-generated αsyn species affects mitochondrial respiration. Mitochondrial dysfunction is a central feature of PD and numerous studies have implicated αsyn in decreasing mitochondrial activity in various animal (Sarafian et al., 2013, Bender et al., 2013, Martin et al., 2006, Li et al., 2013, Zhu et al., 2011, Chinta et al., 2010) and cell culture models of disease (Devi et al., 2008, Reeve et al., 2015, Parihar et al., 2008). In addition to overall decreases in mitochondrial respiration, αsyn has been reported to cause functional deficits, particularly at the level of Complex I. Cells expressing wild-type or mutant αsyn reportedly have deficits in Complex I (Chinta et al., 2010, Devi et al., 2008), which are also observed in post mortem PD brain (Schapira et al., 1989, Parker et al., 1989, Janetzky et al., 1994). Hence the robust hyperactive respiration without functional deficit observed in SH-SY5Y cells in the presence of misfolded αsyn reported in the current study is in contrast to the general paradigm that αsyn decreases mitochondrial respiration in association with Complex I deficiency.

In order to delineate these divergent findings, it is important to consider factors that may contribute to variations in results. A major influence is likely to be the model used, with cell culture systems, transgenic animal models and human disease all harbouring very different cellular environments. Reporting an acute insult to naïve, healthy cells upon treatment with misfolded protein is likely dissimilar to the disease in humans which has been slowly progressing over years of clinical dormancy. Similarly, given that the overexpression of protein in cultured cells does not result in intracellular aggregation of protein, it also is unlike the human condition. In this regard, it could be argued the introduction of misfolded protein into naïve cells is more biologically relevant than a cellular environment where the clearance machinery is adequately removing protein aggregates. Regardless, while each system identifies an effect of αsyn, its relevance to *in vivo* PD is uncertain. However, this also reflects an important point with data collected on human samples, which report the status of mitochondria at post mortem and hence terminal stages of disease. Detailing this stage of disease, while relevant, may not be an adequate representation of mitochondrial health for the majority of the disease process. Considering this, it is possible the mitochondria are able to adapt to the insult caused by αsyn for the majority of the disease course, before being overwhelmed at end-stage disease. Such a scenario would align with the findings of this study. In support of this, numerous studies on mitochondrial respiration in various cell types in small cohorts of ante mortem PD patients have failed to produce conclusive findings (Bravi et al., 1992, Yoshino et al., 1992, Barroso et al., 1993, Martin et al., 1996, Parker and Swerdlow, 1998, Shinde and Pasupathy, 2006, Cronin-Furman et al., 2013, Ambrosi et al., 2014, Esteves et al., 2010). Importantly, recently a larger study examining

mitochondrial respiration in immortalized lymphocytes from 30 patients found enhanced respiratory activity with no functional deficit (Annesley et al., 2016). This elevation was found to be independent of age, disease duration or disease severity and hence supports the theory that mitochondria are adaptive in disease. Collectively, the data presented here and by others suggests the dogma that mitochondria dysfunction is a persistent, overwhelming feature of PD may ultimately be revised.

This work did not elucidate whether the changes in mitochondrial respiratory function upon exposure to misfolded αsyn were due to a direct or indirect mechanism. The observation in Figure 3A-B that PMCA-generated αsyn species selectively associates with CA is support for αsyn modulating mitochondria respiration via a direct interaction with this lipid. CA is commonly referred to as the signature phospholipid of the mitochondrion. It is predominately expressed in the IMM, which contains more than 40 fold higher levels of CA than the outer mitochondrial membrane (OMM) (de Kroon et al., 1997) and is a component of and/or required for the optimal functioning for all major components of the ETC (Paradies et al., 2014). Therefore, consistent with the elevated mitochondrial oxidative phosphorylation reported in this study, if an interaction between αsyn and CA occurs in a biological setting, it would likely result in broad spectrum changes to respiration. Further support for a direct interaction of αsyn with mitochondria comes from many studies showing mutant or wild-type αsyn associates with isolated mitochondria (Parihar et al., 2008, Nakamura et al., 2008) and mitochondria *in vivo* (Devi et al., 2008, Cole et al., 2008, Parihar et al., 2008, Shavali et al., 2008, Chinta et al., 2010). Also, αsyn has been shown to bind to membranes mimicking mitochondrial membranes, with a preference for those containing CA (Zigoneanu et al., 2012, Nakamura et al., 2011).

Given that this current work does not confirm a direct interaction between misfolded αsyn and mitochondria, it is possible that indirect mechanisms are driving the enhanced mitochondrial respiratory activity. As a general rule, enhanced respiration to all complexes without altering function would implicate an indirect mechanism. The most likely candidates for this are those that trigger an increase in ATP production. Autophagic flux is a major modulator of cellular respiration and thus the detection and clearance of misfolded αsyn may be a major contributing pathway to the changes in respiration seen here. However, the finding that glycolysis was unaffected upon exposure to PMCA-generated αsyn reveals important information on the potential mechanism of action. It suggests that if mitochondrial respiration was enhanced because of increased energy demands following exposure to misfolded αsyn, it did not also drive changes in glycolysis. This is consistent with the fact that no mitochondrial deficits were identified and hence glycolysis was not upregulated as a compensatory mechanism. It also eliminates changes to glycolysis as a driver of the effects seen. It should be borne in mind that both the glycolysis and mitochondrial function assays used here were designed to avoid constraints on activity by substrate supply rates. Furthermore, while further analysis is merited,

observing hyperactive mitochondrial respiration following acute exposure of αsyn in this system is likely independent of chronic adaptive pathways.

In conclusion, the aim of this study was to develop a system to produce a heterogeneous population of misfolded αsyn species under non-toxic conditions and to investigate pathogenic mechanisms associated with these species. We show the development and characterization of a protocol to generate αsyn species in the non-toxic buffer PBSN using PMCA. These misfolded species were found to associate with the mitochondrial-specific lipid CA. CA accelerates αsyn fibrillization and alters the formation of αsyn species produced by PMCA. Critically PMCA-generated misfolded αsyn was shown to enhance mitochondrial respiratory activity in neuronal SH-SY5Y cells. This finding is paradigm shifting and may have important implications for our understanding of the pathogenesis of synucleinopathies, including PD.

Materials and methods

Preparation of recombinant protein for αsyn PMCA

The open reading frame of the wild-type human αsyn gene SNCA had previously been cloned into the plasmid pRSET B under the control of the T7 promotor (Cappai et al., 2005). Recombinant human αsyn produced using this plasmid was purchased from Monash Protein Production facility (Monash University Clayton VIC) and supplied as 1 mL aliquots in distilled water (dH_2O). Purchased protein was lyophilized overnight using a benchtop freeze dry system (Labcono, U.S.A) and stored at -80°C until reconstituted in buffer. The following buffers were used in this study: prion conversion buffer (PCB; 1% (v/v) Triton-X 100, 150 mM NaCl, cOmplete ULTRA protease inhibitor cocktail tablet (1 per 10 mL; Roche)/phosphate buffered saline (PBS; Amresco, Solon, OH, U.S.A)), PBS, PBS+150 mM NaCl (PBSN), tris buffered saline (TBS; Amresco, Solon, OH, U.S.A) and TBS+150 mM NaCl (TBSN). For reconstitution of protein, 10 – 16 mg protein was dissolved in 1 mL buffer and centrifuged at 122, 500 *g* for 30 min, 4°C (Optima™ MAX Ultracentrifuge, Beckman Coulter) to sediment amorphous aggregates. Protein concentration of the supernatant was determined by measuring protein absorbance at 280 nm using a photometer (BioPhotometer, Eppendorf) and employing the Beer-Lambert law. Protein was diluted to a final concentration of 90 µM and 60 µL aliquoted into PCR tubes and stored at -80°C until experimental use in αsyn PMCA.

αsyn PMCA

αsyn PMCA was performed as described previously (Herva et al., 2014). PCR tubes containing αsyn were briefly spun in a benchtop centrifuge (Microfuge®16 centrifuge, Beckman Coulter), 37±3 mg

beads (1.0 mm zirconia/silica beads, BioSpec Products) were added and tubes sealed with Parafilm (Pechiney Plastic Packaging Company, Chicago, IL, USA). Samples were placed into a 96-tube rack in a microplate cup-horn sonicator (Misonix 4000) that was filled with water using a circulating water bath to maintain a steady state temperature of 37°C. PMCA reactions using αsyn consisted of 20 sec of sonication every 29 min 40 sec for varying lengths of time. Power setting 7 was used for all αsyn PMCA experiments. For protease resistance studies, PK was diluted in PBSN to 6 x the desired final concentration and 4 µL added to 20 µL of the PMCA product prior to incubation at 37 °C for 30 min with occasional agitation. Replacement of PK with PBSN in equivalent samples acted as non-PK controls and these samples were kept at room temperature (RT) during the digestion of PK-containing samples. All samples were then diluted in 4x NuPAGE LDS sample buffer (Life Technologies) and boiled at 100°C for 10 mins. Samples were resolved using SDS-PAGE and western immunoblot employed to detect αsyn species using the antibody MJFR1 (abcam138501, 1:10,000 dilution) (Brudek et al., 2016).

Thioflavin T (ThT) assay

Extent of fibrillization was quantified in PMCA products by reactivity to ThT (Sigma Aldrich). Here, protein solution was diluted 1/25 in ThT solution (20 µM ThT, 50 mM Glycine in dH_2O, pH 8.5 with KOH) for a final volume of 250 µL in a well of a 96-well black polystyrene plate (Nunc™, Thermo Fisher Scientific). Fluorescence was measured using a Varioskan plate reader (Thermo Fischer Scientific). Triplicate wells of the same sample were averaged and values determined following subtraction of recordings of ThT solution void of sample to account for background fluorescence. When determining the effect of a compound on PMCA-induced αsyn fibrillization using ThT, separate tubes containing the compound in 60 µL of PBSN only was added to PMCA for 72 h, as well as protein containing the compound left at -80°C for the duration of the PMCA. These served as controls to confirm no ThT signal was attributed to the compound in the presence and absence of PMCA. For studies investigating kinetics of αsyn fibrillization, individual PCR tubes of αsyn were placed into the 96-tube rack of a running sonicator that was continuously cycling. This was done at specified intervals to enable all tubes to be removed at the same time such that their total process time corresponded to the time-point of interest.

Transmission electron microscopy

For imaging PMCA products using TEM, samples were applied to formvar-coated grids and visualized by negative staining with uranyl acetate (2% w/v in H_2O), with images captured using a Joel JEM-2100 electron microscope.

Circular dichroism spectroscopy

Conformational changes in αsyn following PMCA were measured using a CD spectrometer (Jasco J-815 CD Spectrometer), with a spectral range of 190 - 260 nm and step size of 1 nm. Analysis was performed using a 1 mm-path length cuvette on protein diluted in dH_2O to a final concentration of 1 mg/mL. CD readings were taken on αsyn protein exposed to PMCA or left at -80ºC (0 h time-point/non-PMCA). The spectrum of buffer alone in an equivalent dilution in dH_2O was also taken to confirm that no inherent spectra came from the PBSN solution.

Lipid binding assays

Lipid strips dotted with 15 long chain (>diC16) highly pure synthetic lipid analogues were purchased from Echelon Inc. and used to determine the affinity of PMCA-generated misfolded or -80ºC monomeric (non-PMCA) αsyn to lipid species. Strips were blocked in 2% skim milk (2 h, RT), prior to incubation with 10 µg/mL αsyn protein diluted in blocking buffer for 2 h, RT. Extent of binding was measured using immunoblot by detection of αsyn using MJFR1 antibody.

Cardiolipin

500 µg of synthetic 16:0 cardiolipin (Echelon, Inc.) was diluted in a small volume of MeOH and solubilized by sonication (Misonix 3000) at 45 ºC, 10 min. Lipid/MeOH was diluted to a final concentration of 1 mg/mL or 0.1 mg/mL and 5 µL added to PCR tubes containing 60 µL of 90 µM αsyn dissolved PBSN.

Transfection of SH-SY5Y cells to produce stable cell lines overexpressing αsyn

In this study, all experiments with cultured cells used SH-SY5Y neuroblastoma cells that were confirmed mycoplasma negative, obtained from American Type Culture Collection (ATCC). To stably overexpress wild-type in SH-SY5Y, the αsyn:pcDNA3+ plasmid was used. SH-SY5Y cells were seeded in complete media (DMEM supplemented with 10% (v/v) fetal calf serum, 1% GlutaMAX (v/v) and 1% penicillin/streptomycin 100 x (v/v); Life Technologies) in a 12-well tissue culture plate at a density of 1.5 x 10^5 for use 48 h later. Cells were serum starved in 750 µL serum free media for 4 h prior to transfection. Varying amounts of plasmid and lipofectamine transfection reagent (Thermo Fisher Scientific) were combined separately in 125 µL Opti-MEM (Thermo Fisher Scientific) per well, before being combined, mixed well and left to incubate for 20 min, RT. 250 µL of the combined solution was then added dropwise to each well and incubated in 37ºC, 5% CO_2 for 6 h

before being replaced with fresh complete media. Cells were left to recover for 48 h before addition of the selective antibiotic G418 (300 µg/mL; Thermo Fisher Scientific) into complete media without added penicillin/streptomycin. Expression of αsyn in clones derived from transfected single cell colonies was monitored by western immunoblot analysis, with the cell line expressing the highest level of αsyn used for further experiments. The αsyn overexpressing SH-SY5Y cell line used in this study was derived from clone A4, and hence named as such.

Lactate dehydrogenase (LDH) cytotoxicity assay

A lactate dehydrogenase (LDH) cytotoxicity assay kit (Thermo Fisher Scientific) was used to determine the cytotoxicity of buffers used in PMCA to A4 and untransfected SH-SY5Y cells. The protocol followed was as per the manufacturer's instructions. Briefly, 1 x 10^4 cells were seeded into a 96-well tissue culture plate and 24 h later triplicate wells were treated with 10 µL of PBSN or PCB diluted in dH_2O to achieve a final concentration of 0.5, 1, 5, or 10% final volume of buffer. Additionally, one set of triplicate wells was treated with dH_2O to act as a control for spontaneous cell death and one set was left untreated to be treated later with lysis buffer to measure maximum cell death (maximum LDH activity). Cells were incubated under standard cell culture conditions for 24 h. Following incubation, 10 µL lysis buffer was added to the set of untreated triplicate wells and incubated again for a further 45 min. 50 µL of media from all wells was then transferred to a 96-well flat-bottom plate. Reaction mixture (50 µL) was added to each well and incubated for 30 min RT protected from light followed by the addition of 50 µL of stop solution. Absorbance was measured at 490 nm and 680 nm to obtain sample fluorescence and background fluorescence, respectively. To determine LDH activity, the 680 nm absorbance was subtracted from the 490 nm value. Percent cytotoxicity of a sample was determined using the formula:

$$\% \text{ toxicity} = \frac{(\text{sample LDH activity} - \text{spontaneous LDH activity})}{(\text{maximum LDH activity} - \text{spontaneous LDH activity})} * 100$$

Western immunoblot of cell lysates

All steps to lyse cultured cells were performed on ice using pre-chilled reagents. Pelleted cells were washed twice with cold PBS and resuspended in lysis buffer (150 mM NaCl, 50 mM Tris pH 7.4, 1% (v/v) Triton X-100, 1% (w/v) sodium deoxycholate (Sigma-Aldrich) and cOmplete ULTRA protease inhibitor in dH_2O). Cells were left to lyse for 20 min with occasional agitation, then unwanted debris and nuclear material removed by centrifugation (1, 000 g, 3 min). The supernatant was collected and

either used immediately in protein determination and western immunoblot analysis, or stored at -80ºC for future use. Immunodetection of αsyn was performed using MJFR1 antibody.

Detection of αsyn in transfected SH-SY5Y cells using immunofluorescence

3 x 10^4 A4 and untransfected SH-SY5Y cells were seeded into 8-well Lab-Tek®II Chamber Slides (Nalge Nunc, Naperville, IL, U.S.A) and left for 48 h to strongly adhere. Cells were washed once in PBS and fixed with 4% (w/v) paraformaldehyde (PFA; Sigma-Aldrich) in PBS for 15 min, RT. Cells were washed three times in PBS to remove residual PFA and permeabilized in 0.5% (v/v) Triton X-100/PBS for 2 min, RT. Cells were washed again as described above and blocked in buffer (2% (w/v) bovine serum albumin (BSA; Sigma-Aldrich)/PBS) for 30 min, RT. Blocking buffer was removed and cells incubated with primary antibody (MJFR1 to detect αsyn) diluted in blocking buffer for 2 h, RT, followed by five washes in PBS. Fluorophore-conjugated (anti-rabbit, 568-Alexa Fluor conjugated) secondary antibody and 4',6-diamidino-2-phenylindole (DAPI), also diluted in blocking buffer were then added to the chamber wells and left for 2 h, RT before a final five washes in PBS. Walls of the chamber slide were removed and mounted with glass cover slips (Mediglass, Taren Point, NSW, Australia) with ProLong™ Gold Antifade Mountant (Thermo-Fisher). Slides were inverted and left to dry overnight in the dark before being sealed with nail polish (Sally Hansen). Images were taken on a SP5 (Leica Microsystems Pty Ltd) confocal microscope.

Preparation of samples for measuring cellular readouts using the Seahorse XFe24 Analyzer

When preparing αsyn and buffer control treatment samples for experiments using the Seahorse XFe24 Analyzer, autoclaved beads were used, and PBSN samples were generated by adding buffer (60 µL) to PCR tubes along with beads (equivalent to the setup with PMCA generated misfolded αsyn), and were similarly exposed to PMCA for 72 h. Confluent SH-SY5Y cells grown in T75 flasks were harvested, pelleted and resuspended in XF assay medium (unbuffered DMEM supplemented with 2.5 mM glucose and 1 mM sodium pyruvate). PMCA-generated misfolded and monomeric (-80ºC) αsyn protein or PBSN only (26.25 µL per well) was mixed with lipofectamine (3 µL per well) and the combined solution added to the cells (2 x 10^5 cells per well) in suspension and mixed gently. Equivalent cell densities were similarly left untreated. Cells and protein (525 µL in total) were then plated into the well of a Seahorse XFe24 plate that had been pre-coated (and subsequently air dried) with Matrigel (356231, Corning) diluted 1:2 in XF assay medium. Cells were left to adhere for 1 h at 37ºC prior to analysis with the Seahorse XFe24 Analyzer with readouts calculated as per 200,000 cells.

Measuring mitochondrial respiratory function in SH-SY5Y cells

Mitochondrial respiratory function in live SH-SY5Y cells was measured using the Seahorse XFe24 Extracellular Flux Analyzer (Seahorse Bioscience) via changes in the oxygen consumption rate (OCR) following the sequential addition of pharmacological agents (2 µM oligomycin, 1 µM CCCP, 5 µM rotenone, 1 µM antimycin A). Between each compound treatment, the average of three measurement cycles of OCR was taken, each cycle including a 3 min mix step, 2 min wait and a measurement time of 3 min. Each condition tested had a minimum of three replicate wells, with the average of the values taken per experiment. Equipment setup for glycolysis measurements was as per respiratory function experiments and glycolytic function determined from changes in pH associated with the extracellular acidification rate (ECAR) in live SH-SY5Y cells. This was measured following the successive addition of pharmacological agents (10 mM glucose, 2 µM oligomycin, 5 µM rotenone 5 µM & antimycin A, 100 mM 2-deoxy-D glucose).

Data analysis

Densitometric analysis was performed on unsaturated western immunoblot images using Image Lab. All statistical analysis was performed using GraphPad Prism, using a statistical criterion of 0.05. Normality was assessed on all samples subjected to statistical analysis to ensure data met the assumptions of the tests used and statistical outliers identified using ROUT method. When values from at least three independent replicates were combined, they were depicted as mean±standard error of the mean (SEM).

Acknowledgements

The authors wish to acknowledge Peter Lock, Ben Scicluna and Irene Volitakis for technical contributions to this manuscript. Roberto Cappai kindly supplied both αsyn constructs (αsyn:pcDNA3+ and αsyn:pRSET B) used in the project. The TEM images were obtained with the help of the Bioimaging Platform (La Trobe University) and the Biological Optical Microscopy Platform (The University of Melbourne). This work was supported by the National Health and Medical Research Council (628946 to AFH). CLU is supported by the Carol Willesee PhD Scholarship at The University of Melbourne.

Competing interests

The authors have no competing or financial interests to declare.

References

AMBROSI, G., GHEZZI, C., SEPE, S., MILANESE, C., PAYAN-GOMEZ, C., BOMBARDIERI, C. R., ARMENTERO, M.-T., ZANGAGLIA, R., PACCHETTI, C., MASTROBERARDINO, P. G. & BLANDINI, F. 2014. Bioenergetic and proteolytic defects in fibroblasts from patients with sporadic Parkinson's disease. *Biochimica Et Biophysica Acta-Molecular Basis of Disease,* 1842**,** 1385-1394.

ANNESLEY, S. J., LAY, S. T., DE PIAZZA, S. W., SANISLAV, O., HAMMERSLEY, E., ALLAN, C. Y., FRANCIONE, L. M., BUI, M. Q., CHEN, Z. P., NGOEI, K. R. W., TASSONE, F., KEMP, B. E., STOREY, E., EVANS, A., LOESCH, D. Z. & FISHER, P. R. 2016. Immortalized Parkinson's disease lymphocytes have enhanced mitochondrial respiratory activity. *Disease Models & Mechanisms,* 9**,** 1295-1305.

APPEL-CRESSWELL, S., VILARINO-GUELL, C., ENCARNACION, M., SHERMAN, H., YU, I., SHAH, B., WEIR, D., THOMPSON, C., SZU-TU, C., TRINH, J., AASLY, J. O., RAJPUT, A., RAJPUT, A. H., STOESSL, A. J. & FARRER, M. J. 2013. α-synuclein p.H50Q, a novel pathogenic mutation for Parkinson's disease. *Movement Disorders,* 28**,** 811-813.

BARROSO, N., CAMPOS, Y., HUERTAS, R., ESTEBAN, J., MOLINA, J. A., ALONSO, A., GUTIERREZRIVAS, E. & ARENAS, J. 1993. Respiratory chain enzyme activities in lymphocytes from untreated patients with Parkinson's disease. *Clinical Chemistry,* 39**,** 667-669.

BENDER, A., DESPLATS, P., SPENCER, B., ROCKENSTEIN, E., ADAME, A., ELSTNER, M., LAUB, C., MUELLER, S., KOOB, A. O., MANTE, M., PHAM, E., KLOPSTOCK, T. & MASLIAH, E. 2013. TOM40 mediates mitochondrial dysfunction induced by α-synuclein accumulation in Parkinson's disease. *Plos One,* 8.

BHARATHI, INDI, S. S. & RAO, K. S. J. 2007. Copper- and iron-induced differential fibril formation in α-synuclein: TEM study. *Neuroscience Letters,* 424**,** 78-82.

BIANCALANA, M. & KOIDE, S. 2010. Molecular mechanism of Thioflavin-T binding to amyloid fibrils. *Biochimica Et Biophysica Acta-Proteins and Proteomics,* 1804**,** 1405-1412.

BRAVI, D., ANDERSON, J. J., DAGANI, F., DAVIS, T. L., FERRARI, R., GILLESPIE, M. & CHASE, T. N. 1992. Effect of aging and dopaminomimetic therapy on mitochondrial respiratory function in Parkinson's disease. *Movement Disorders,* 7**,** 228-231.

BRUDEK, T., WINGE, K., RASMUSSEN, N. B., BAHL, J. M., TANASSI, J., AGANDER, T. K., HYDE, T. M. & PAKKENBERG, B. 2016. Altered α-synuclein, parkin, and synphilin isoform levels in multiple system atrophy brains. *J Neurochem,* 136**,** 172-85.

CAPPAI, R., LECK, S.-L., TEW, D. J., WILLIAMSON, N. A., SMITH, D. P., GALATIS, D., SHARPLES, R. A., CURTAIN, C. C., ALI, F. E., CHERNY, R. A., CULVENOR, J. G., BOTTOMLEY, S. P., MASTERS, C. L., BARNHAM, K. J. & HILL, A. F. 2005. Dopamine promotes α-synuclein aggregation into SDS-resistant soluble oligomers via a distinct folding pathway. *FASEB journal*.

CHARTIER-HARLIN, M. C., KACHERGUS, J., ROUMIER, C., MOUROUX, V., DOUAY, X., LINCOLN, S., LEVECQUE, C., LARVOR, L., ANDRIEUX, J., HULIHAN, M., WAUCQUIER, N., DEFEBVRE, L., AMOUYEL, P., FARRER, M. & DESTEE, A. 2004. α-synuclein locus duplication as a cause of familial Parkinson's disease. *Lancet,* 364**,** 1167-1169.

CHINTA, S. J., MALLAJOSYULA, J. K., RANE, A. & ANDERSEN, J. K. 2010. Mitochondrial α-synuclein accumulation impairs complex I function in dopaminergic neurons and results in increased mitophagy *in vivo*. *Neuroscience Letters,* 486**,** 235-239.

COLE, N. B., DIEULIIS, D., LEO, P., MITCHELL, D. C. & NUSSBAUM, R. L. 2008. Mitochondrial translocation of α-synuclein is promoted by intracellular acidification. *Experimental Cell Research,* 314**,** 2076-2089.

CREMADES, N., COHEN, SAMUEL I., DEAS, E., ABRAMOV, ANDREY Y., CHEN, ALLEN Y., ORTE, A., SANDAL, M., CLARKE, RICHARD W., DUNNE, P., APRILE,

FRANCESCO A., BERTONCINI, CARLOS W., WOOD, NICHOLAS W., KNOWLES, TUOMAS P., DOBSON, CHRISTOPHER M. & KLENERMAN, D. 2012. Direct observation of the interconversion of normal and toxic forms of α-synuclein. *Cell,* 149**,** 1048-1059.

CRONIN-FURMAN, E. N., BORLAND, M. K., BERGQUIST, K. E., BENNETT, J. P., JR. & TRIMMER, P. A. 2013. Mitochondrial quality, dynamics and functional capacity in Parkinson's disease cybrid cell lines selected for Lewy body expression. *Molecular Neurodegeneration,* 8.

DE KROON, A., DOLIS, D., MAYER, A., LILL, R. & DEKRUIJFF, B. 1997. Phospholipid composition of highly purified mitochondrial outer membranes of rat liver and Neurospora crassa. Is cardiolipin present in the mitochondrial outer membrane? *Biochimica Et Biophysica Acta-Biomembranes,* 1325**,** 108-116.

DEVI, L., RAGHAVENDRAN, V., PRABHU, B. M., AVADHANI, N. G. & ANANDATHEERTHAVARADA, H. K. 2008. Mitochondrial import and accumulation of α-synuclein impair complex I in human dopaminergic neuronal cultures and Parkinson disease brain. *Journal of Biological Chemistry,* 283**,** 9089-9100.

ESTEVES, A. R., LU, J., RODOVA, M., ONYANGO, I., LEZI, E., DUBINSKY, R., LYONS, K. E., PAHWA, R., BURNS, J. M., CARDOSO, S. M. & SWERDLOW, R. H. 2010. Mitochondrial respiration and respiration-associated proteins in cell lines created through Parkinson's subject mitochondrial transfer. *Journal of Neurochemistry,* 113**,** 674-682.

GALVIN, J. E., LEE, V. M. & TROJANOWSKI, J. Q. 2001. Synucleinopathies: clinical and pathological implications. *Arch Neurol,* 58**,** 186-90.

GARCIA-ESPARCIA, P., HERNANDEZ-ORTEGA, K., KONETI, A., GIL, L., DELGADO-MORALES, R., CASTANO, E., CARMONA, M. & FERRER, I. 2015. Altered machinery of protein synthesis is region- and stage-dependent and is associated with α-synuclein oligomers in Parkinson's disease. *Acta Neuropathol Commun,* 3**,** 76.

HERVA, M. E., ZIBAEE, S., FRASER, G., BARKER, R. A., GOEDERT, M. & SPILLANTINI, M. G. 2014. Anti-amyloid compounds inhibit α-synuclein aggregation induced by protein misfolding cyclic amplification (PMCA). *The Journal Of Biological Chemistry*.

JANETZKY, B., HAUCK, S., YOUDIM, M. B. H., RIEDERER, P., JELLINGER, K., PANTUCEK, F., ZOCHLING, R., BOISSL, K. W. & REICHMANN, H. 1994. Unaltered aconitase activity, but decreased complex I activity in substantia nigra pars compacta of patients with Parkinson's disease. *Neuroscience Letters,* 169**,** 126-128.

KRUGER, R., KUHN, W., MULLER, T., WOITALLA, D., GRAEBER, M., KOSEL, S., PRZUNTEK, H., EPPLEN, J. T., SCHOLS, L. & RIESS, O. 1998. Ala30Pro mutation in the gene encoding α-synuclein in Parkinson's disease. *Nature Genetics,* 18**,** 106-108.

LESAGE, S., ANHEIM, M., LETOURNEL, F., BOUSSET, L., HONORE, A., ROZAS, N., PIERI, L., MADIONA, K., DURR, A., MELKI, R., VERNY, C., BRICE, A. & FRENCH PARKINSONS DIS GENET, S. 2013. G51D α-synuclein mutation causes a novel Parkinsonian-pyramidal syndrome. *Annals of Neurology,* 73**,** 459-471.

LI, L., NADANACIVA, S., BERGER, Z., SHEN, W., PAUMIER, K., SCHWARTZ, J., MOU, K., LOOS, P., MILICI, A. J., DUNLOP, J. & HIRST, W. D. 2013. Human A53T α-synuclein causes reversible deficits in mitochondrial function and dynamics in primary mouse cortical neurons. *Plos One,* 8.

MARTIN, L. J., PAN, Y., PRICE, A. C., STERLING, W., COPELAND, N. G., JENKINS, N. A., PRICE, D. L. & LEE, M. K. 2006. Parkinson's disease α-synuclein transgenic mice develop neuronal mitochondrial degeneration and cell death. *Journal of Neuroscience,* 26**,** 41-50.

MARTIN, M. A., MOLINA, J. A., JIMENEZJIMENEZ, F. J., BENITOLEON, J., ORTIPAREJA, M., CAMPOS, Y., ARENAS, J., ALVAREZCERMENO, J. C., ARCAYA, J., AYUSOPERALTA, L., BALSEIRO, J., BERMEJO, F., CAMINERO, A., CATALAN, M. J., CEBALLOS, A., DOMINGO, J., DUARTE, J., FERNANDEZCARRIL, J. M., GALIANO, M., GARCIARUIZ, P. J., GARCIAURRA, D., GIMENEZROLDAN, S., GRANDAS, F., LOPEZLOZANO, J. J., LUENGO, A., MARCO, J., MARSAL, C., MARTINEZMARTIN, P., MATEO, D., MUNOZVAZQUEZ, A., NOS, J., PEREZSEMPERE, A., PONDALSORDO, M., PUENTESGIL, J. M., RABASA, M., RALLOGUTIERREZ, B.,

RIVAMEANA, C., RUIZEZQUERRO, J. J., SANCHEZALONSO, P., SANCHEZPERNAUTE, R., TABERNERO, C., VAAMONDE, J., VAQUEZ, A., VELADESOJO, L., VIVANCOSMATELLANO, F., DEYEBENES, J. G. & YUSTA, A. 1996. Respiratory-chain enzyme activities in isolated mitochondria of lymphocytes from untreated Parkinson's disease patients. *Neurology,* 46**,** 1343-1346.

MUNISHKINA, L. A., FINK, A. L. & UVERSKY, V. N. 2008. Concerted action of metals and macromolecular crowding on the fibrillation of α-synuclein. *Protein and Peptide Letters,* 15**,** 1079-1085.

NAKAMURA, K., NEMANI, V. M., AZARBAL, F., SKIBINSKI, G., LEVY, J. M., EGAMI, K., MUNISHKINA, L., ZHANG, J., GARDNER, B., WAKABAYASHI, J., SESAKI, H., CHENG, Y. F., FINKBEINER, S., NUSSBAUM, R. L., MASLIAH, E. & EDWARDS, R. H. 2011. Direct membrane association drives mitochondrial fission by the Parkinson disease-associated protein α-synuclein. *Journal of Biological Chemistry,* 286**,** 20710-20726.

NAKAMURA, K., NEMANI, V. M., WALLENDER, E. K., KAEHLCKE, K., OTT, M. & EDWARDS, R. H. 2008. Optical reporters for the conformation of α-synuclein reveal a specific interaction with mitochondria. *Journal of Neuroscience,* 28**,** 12305-12317.

PARADIES, G., PARADIES, V., DE BENEDICTIS, V., RUGGIERO, F. M. & PETROSILLO, G. 2014. Functional role of cardiolipin in mitochondrial bioenergetics. *Biochim Biophys Acta,* 1837**,** 408-17.

PARIHAR, M. S., PARIHAR, A., FUJITA, M., HASHIMOTO, M. & GHAFOURIFAR, P. 2008. Mitochondrial association of α-synuclein causes oxidative stress. *Cellular and Molecular Life Sciences,* 65**,** 1272-1284.

PARKER, W. D., BOYSON, S. J. & PARKS, J. K. 1989. Abnormalities of the electron transport chain in idiopathic Parkinson's disease. *Annals of Neurology,* 26**,** 719-723.

PARKER, W. D. & SWERDLOW, R. H. 1998. Mitochondrial dysfunction in idiopathic Parkinson disease. *American Journal of Human Genetics,* 62**,** 758-762.

POLYMEROPOULOS, M. H., LAVEDAN, C., LEROY, E., IDE, S. E., DEHEJIA, A., DUTRA, A., PIKE, B., ROOT, H., RUBENSTEIN, J., BOYER, R., STENROOS, E. S., CHANDRASEKHARAPPA, S., ATHANASSIADOU, A., PAPAPETROPOULOS, T., JOHNSON, W. G., LAZZARINI, A. M., DUVOISIN, R. C., DIIORIO, G., GOLBE, L. I. & NUSSBAUM, R. L. 1997. Mutation in the α-synuclein gene identified in families with Parkinson's disease. *Science,* 276**,** 2045-2047.

PROUKAKIS, C., DUDZIK, C. G., BRIER, T., MACKAY, D. S., COOPER, J. M., MILLHAUSER, G. L., HOULDEN, H. & SCHAPIRA, A. H. 2013. A novel α-synuclein missense mutation in Parkinson disease. *Neurology,* 80**,** 1062-1064.

REEVE, A. K., LUDTMANN, M. H. R., ANGELOVA, P. R., SIMCOX, E. M., HORROCKS, M. H., KLENERMAN, D., GANDHI, S., TURNBULL, D. M. & ABRAMOV, A. Y. 2015. Aggregated α-synuclein and complex I deficiency: exploration of their relationship in differentiated neurons. *Cell Death & Disease,* 6**,** e1820-e1820.

ROBERTS, H. L. & BROWN, D. R. 2015. Seeking a mechanism for the toxicity of oligomeric α-synuclein. *Biomolecules,* 5**,** 282-305.

SABORIO, G. P., PERMANNE, B. & SOTO, C. 2001. Sensitive detection of pathological prion protein by cyclic amplification of protein misfolding. *Nature,* 411**,** 810-813.

SARAFIAN, T. A., RYAN, C. M., SOUDA, P., MASLIAH, E., KAR, U. K., VINTERS, H. V., MATHERN, G. W., FAULL, K. F., WHITELEGGE, J. P. & WATSON, J. B. 2013. Impairment of mitochondria in adult mouse brain overexpressing predominantly full-length, N-terminally acetylated human α-synuclein. *Plos One,* 8.

SCHAPIRA, A. H. V., COOPER, J. M., DEXTER, D., JENNER, P., CLARK, J. B. & MARSDEN, C. D. 1989. Mitochondrial complex I deficiency in Parkinson's disease. *Lancet,* 1**,** 1269-1269.

SHARON, R., BAR-JOSEPH, I., FROSCH, M. P., WALSH, D. M., HAMILTON, J. A. & SELKOE, D. J. 2003. The formation of highly soluble oligomers of α-synuclein is regulated by fatty acids and enhanced in Parkinson's disease. *Neuron,* 37**,** 583-595.

SHAVALI, S., BROWN-BORG, H. M., EBADI, M. & PORTER, J. 2008. Mitochondrial localization of α-synuclein protein in α-synuclein overexpressing cells. *Neuroscience Letters,* 439**,** 125-128.

SHINDE, S. & PASUPATHY, K. 2006. Respiratory-chain enzyme activities in isolated mitochondria of lymphocytes from patients with Parkinson's disease: Preliminary study. *Neurology India,* 54**,** 390-393.

SINGLETON, A. B., FARRER, M., JOHNSON, J., SINGLETON, A., HAGUE, S., KACHERGUS, J., HULIHAN, M., PEURALINNA, T., DUTRA, A., NUSSBAUM, R., LINCOLN, S., CRAWLEY, A., HANSON, M., MARAGANORE, D., ADLER, C., COOKSON, M. R., MUENTER, M., BAPTISTA, M., MILLER, D., BLANCATO, J., HARDY, J. & GWINN-HARDY, K. 2003. α-synuclein locus triplication causes Parkinson's disease. *Science,* 302**,** 841-841.

SURMEIER, D. J., OBESO, J. A. & HALLIDAY, G. M. 2017. Selective neuronal vulnerability in Parkinson disease. *Nat Rev Neurosci,* 18**,** 101-113.

TOFARIS, G. K., RAZZAQ, A., GHETTI, B., LILLEY, K. S. & SPILLANTINI, M. G. 2003. Ubiquitination of α-synuclein in Lewy bodies is a pathological event not associated with impairment of proteasome function. *Journal of Biological Chemistry,* 278**,** 44405-44411.

UGALDE, C. L., FINKELSTEIN, D. I., LAWSON, V. A. & HILL, A. F. 2016. Pathogenic mechanisms of prion protein, amyloid-β and α-synuclein misfolding: the prion concept and neurotoxicity of protein oligomers. *J Neurochem,* 139**,** 162-180.

UGALDE, C. L., LAWSON, V. A., FINKELSTEIN, D. I. & HILL, A. F. 2019. The role of lipids in α-synuclein misfolding and neurotoxicity. *The Journal Of Biological Chemistry*.

UVERSKY, V. N., LI, J. & FINK, A. L. 2001. Metal-triggered structural transformations, aggregation, and fibrillation of human α-synuclein - a possible molecular link between Parkinson's disease and heavy metal exposure. *Journal of Biological Chemistry,* 276**,** 44284-44296.

VASSAR, P. S. & CULLING, C. F. A. 1959. Fluorescent stains, with special reference to amyloid and connective tissue. *Archives of Pathology,* 68**,** 487-498.

YOSHINO, H., NAKAGAWAHATTORI, Y., KONDO, T. & MIZUNO, Y. 1992. Mitochondrial complex I and complex II activities of lymphocytes and platelets in Parkinson's disease. *Journal of Neural Transmission-Parkinsons Disease and Dementia Section,* 4**,** 27-34.

ZARRANZ, J. J., ALEGRE, J., GOMEZ-ESTEBAN, J. C., LEZCANO, E., ROS, R., AMPUERO, I., VIDAL, L., HOENICKA, J., RODRIGUEZ, O., ATARES, B., LLORENS, V., TORTOSA, E. G., DEL SER, T., MUNOZ, D. G. & DE YEBENES, J. G. 2004. The new mutation, E46K, of α-synuclein causes Parkinson and Lewy body dementia. *Annals of Neurology,* 55**,** 164-173.

ZHU, Y. G., DUAN, C. L., LU, L., GAO, H., ZHAO, C. L., YU, S., UEDA, K., CHAN, P. & YANG, H. 2011. α-synuclein overexpression impairs mitochondrial function by associating with adenylate translocator. *International Journal of Biochemistry & Cell Biology,* 43**,** 732-741.

ZIGONEANU, I. G., YANG, Y. J., KROIS, A. S., HAQUE, M. E. & PIELAK, G. J. 2012. Interaction of α-synuclein with vesicles that mimic mitochondrial membranes. *Biochimica Et Biophysica Acta-Biomembranes,* 1818**,** 512-519.

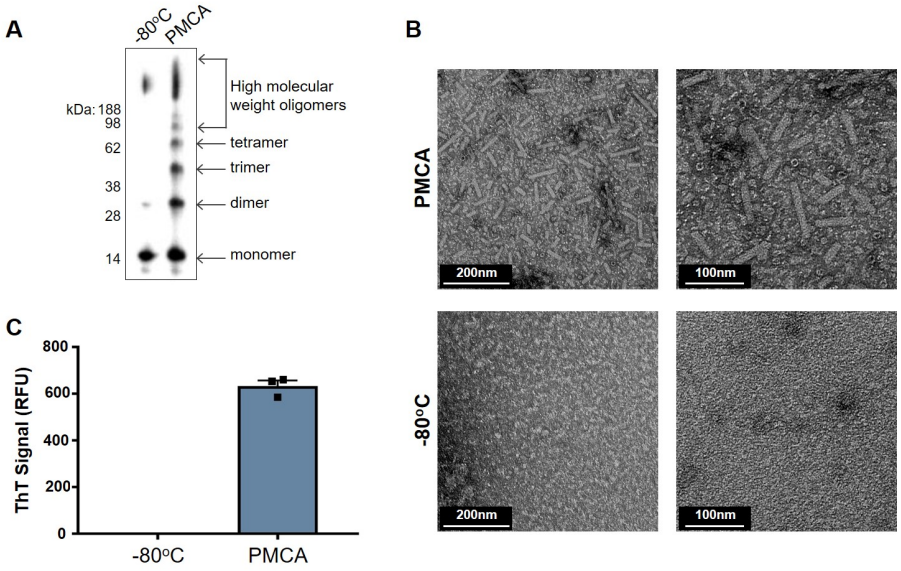

Figure 1: αsyn PMCA. Extent of fibrillization in protein exposed to PMCA and non-PMCA controls (-80ºC) was assessed by (A) western immunoblot analysis using αsyn-specific monoclonal antibody MJFR1 (amino acid specificity: 118-123) (B) transmission electron microscopy (representative images) and (C) ThT fluorescence, where the values obtained for each experimental replicate represented the average fluorescence of triplicate wells after subtraction of a blank well to account for background fluorescence (RFU= relative fluorescent units). Data presented as mean±SEM (n=3) and represent every experimental replicate performed.

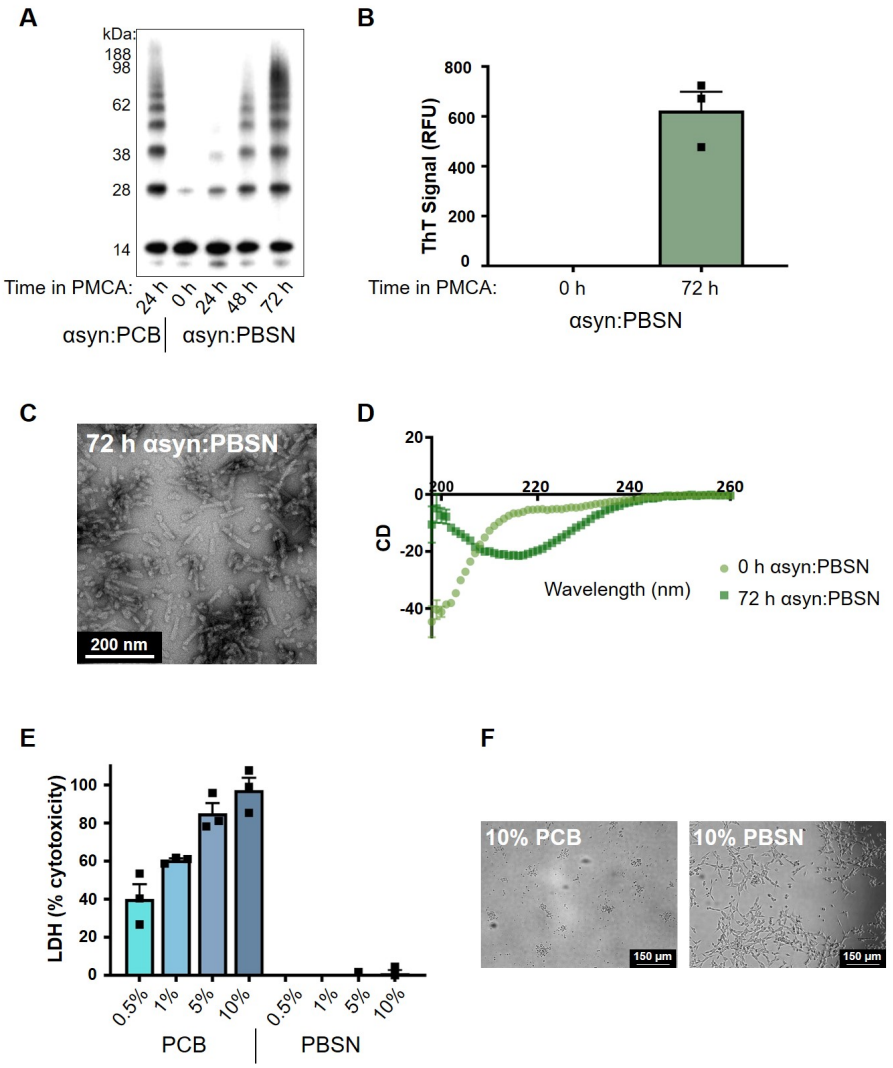

Figure 2: Production of misfolded αsyn species in PBSN buffer produces comparable misfolded content to αsyn species generated in prion conversion buffer (PCB). Lyophilized recombinant wild-type protein was reconstituted in PBSN (αsyn:PBSN) or PCB (αsyn:PCB) and subjected to PMCA for a total process time of 0, 24, 48 or 72 h. (A) Extent of fibrillization in samples was assessed using western immunoblot analysis using αsyn-specific monoclonal antibody MJFR1 (amino acid specificity: 118-123). (B) αsyn:PBSN exposed to PMCA for 72 h or non-PMCA (0 h) monomeric controls were further characterized by ThT fluorescence, where the values obtained for each experimental replicate represented the average fluorescence of triplicate wells after subtraction of a blank well to account for background fluorescence (RFU= relative fluorescent units). Data presented as mean±SEM (n=3) and represent every experimental replicate performed. (C) Transmission electron microscopy of fibrils produced in PBSN after 72 h PMCA (representative image). (D) Secondary structure of 0 h and 72 h PMCA αsyn:PBSN was determined using circular dichroism (CD) spectroscopy (n=1, representative spectra). (E) Toxicity of PCB and PBSN in SH-SY5Y cells after 24 h was measured by assessing LDH levels via absorbance. Values were expressed as a percent cytotoxicity compared to equivalent cells treated with lysis buffer (maximum cell death). Deduction of water treated samples accounted for spontaneous LDH release. All buffers were measured using triplicate reads. Data presented as mean±SEM (n=3) and represent every experimental replicate performed. (F) Following treatment with PBSN or PCB differential interference contrast (DIC) images of cells were taken. n=1, representative images.

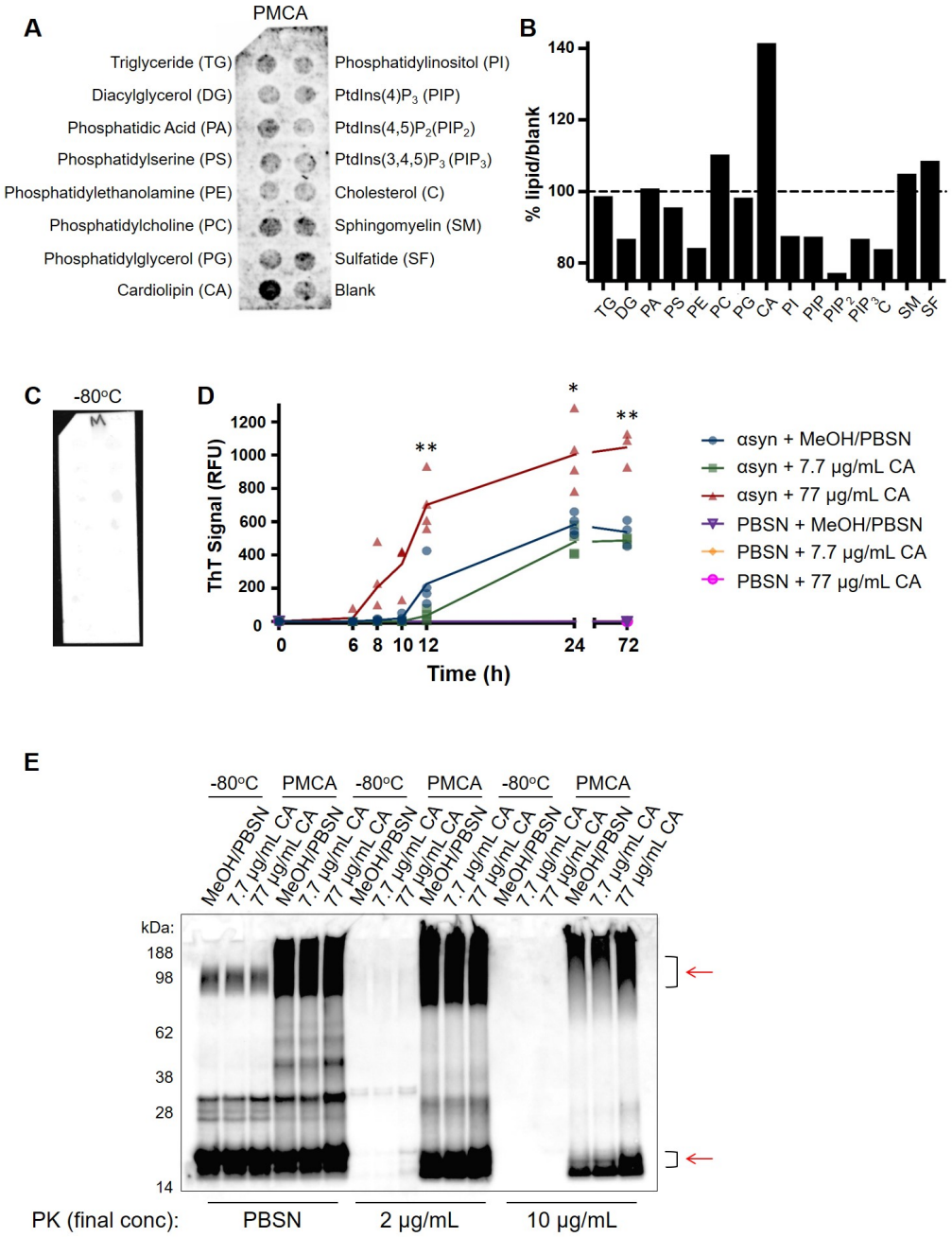

Figure 3: PMCA-generated αsyn selectively associates with cardiolipin (CA). A hydrophobic membrane strip dotted with 15 different lipids (long-chain >diC16 synthetic analogues) was incubated with PMCA-generated αsyn (A) Binding of αsyn to lipids was assessed via western immunoblot using αsyn-specific monoclonal antibody MJFR1 (amino acid specificity: 118-123). (B) Extent of binding was quantified as % over blank. (C) Unlike PMCA-generated misfolded αsyn, monomeric αsyn (-80ºC) did not show affinity to any lipid class, n=1. To determine if cardiolipin (CA) modulates αsyn fibrillization, CA was dissolved in MeOH/PBSN and added to wild-type αsyn for a final concentration of 7.7 and 77 µg/mL CA. MeOH/PBSN alone added to αsyn:PBSN served to control for the effect of the buffer. (D) Samples were subjected to PMCA for a total process time of 0, 6, 8, 10, 12, 24 and 72 h. Tubes containing PBSN only (no αsyn) with buffer or CA exposed to PMCA for 0 and 72 h served to detect any inherent fluorescence caused by CA or the buffer. Extent of fibrillization was assessed by measuring ThT fluorescence, where the values obtained for each experimental replicate represented the average fluorescence of triplicate wells after subtraction of a blank well to account for background fluorescence (RFU= relative fluorescent units). Data presented as mean±SEM (n=4 for all groups except for 0 h and 72 h which were n=3) and represent every experimental replicate performed. To determine the effect of CA on αsyn fibrillization compared to control samples, a mixed-effects ANOVA with Dunnett's multiple comparisons test was employed *p<0.05, **p<0.01 (E) The biochemical properties of αsyn species formed after 72 h PMCA (PMCA) or not (-80ºC) was assessed by its resistance to proteolysis following digestion in proteinase K (PK) at final concentration of 0, 2 or 10 µg/mL. PK-resistant species were detected by immunoblot using MJFR1. Areas of differential PK resistance between PMCA-generated species are identified by red arrows. n=1.

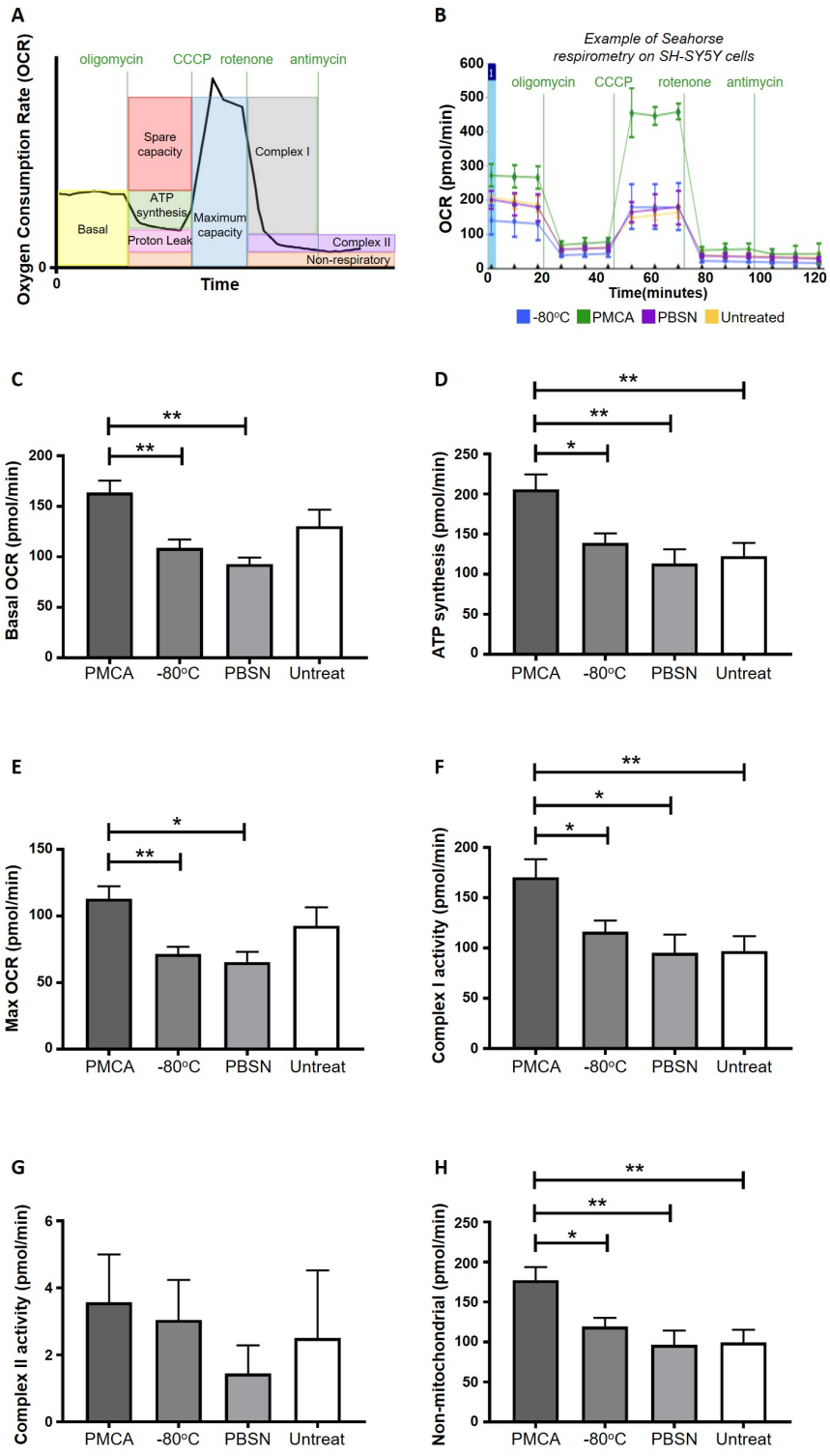

Figure 4: PMCA-generated misfolded αsyn causes mitochondrial respiration to become hyperactive in SH-SY5Y cells. SH-SY5Y cells were incubated with PMCA-generated αsyn, monomeric αsyn (-80°C), buffer alone (PBSN) or left untreated (Untreat). Media-containing cells were plated into a well of a Seahorse XFe24 plate and mitochondria respiration measured in adhered cells using the Seahorse XF Analyzer. This was performed by detecting changes in oxygen (referred to as the oxygen consumption rate; OCR) following the addition of pharmacological agents: oligomycin, carbonyl cyanide m-chlorophenyl hydrazone (CCCP), rotenone and antimycin A. In doing so, the following parameters were measured: (C) basal OCR, (D) ATP synthesis, (E) max OCR, (F) complex I activity, (G) complex II activity and (H) non-mitochondrial respiration. The average of five wells was taken for each sample per experimental replicate. Data presented as mean±SEM (n=15, 15, 7, 12 for groups PMCA, -80°C, PBSN and Untreat, respectively) and represent every experimental replicate performed. Statistical significance was examined by ANOVA and Tukey's multiple comparisons test with a statistical criterion of 0.05. *p<0.05, **p<0.01

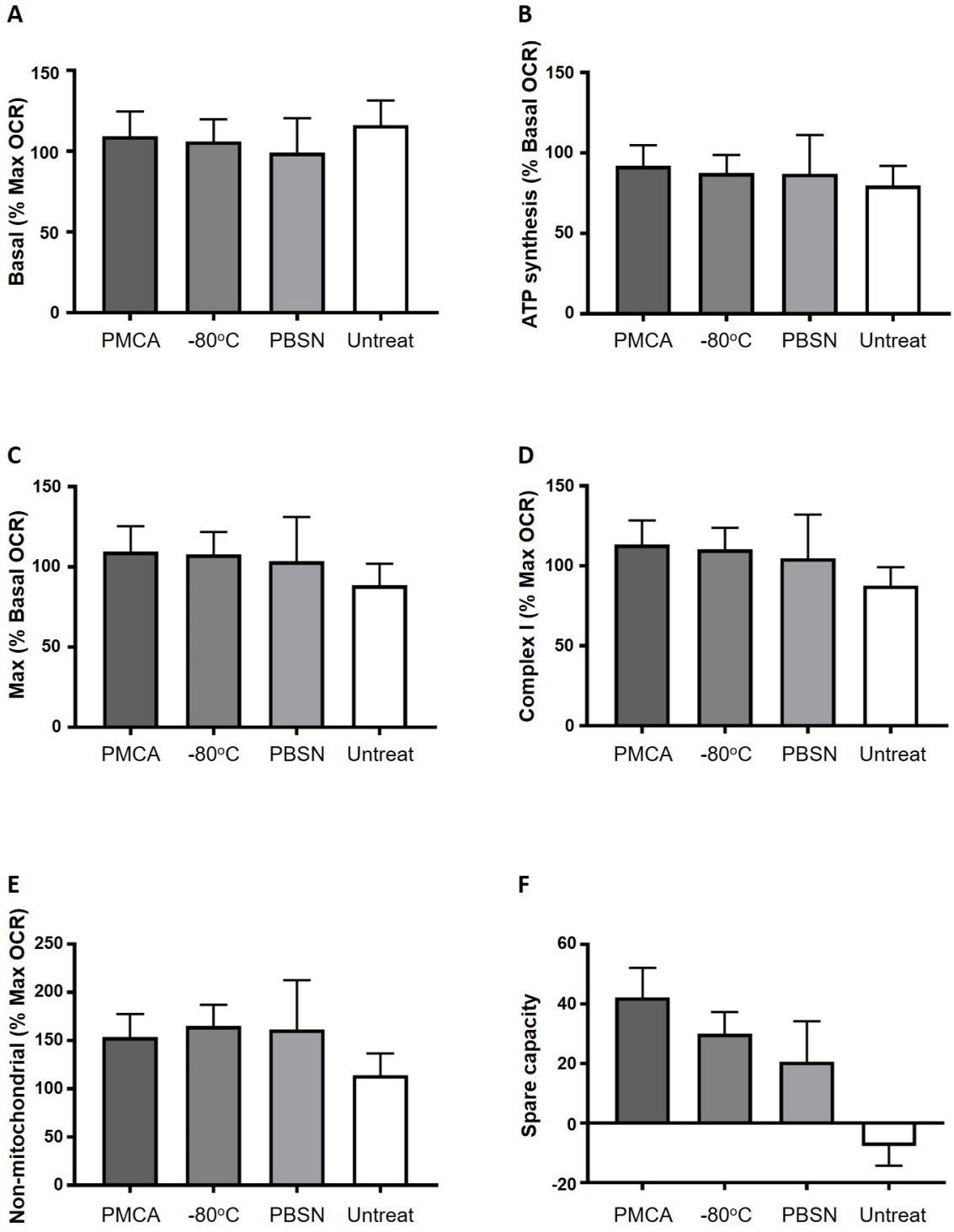

Figure 5: PMCA-generated misfolded αsyn do not cause functional deficits in mitochondria of SH-SY5Y cells. SH-SY5Y cells were incubated with PMCA-generated αsyn, monomeric αsyn (-80°C), buffer alone (PBSN) or left untreated (Untreat). Media-containing cells were plated into a well of a Seahorse XFe24 plate pre-coated with Matrigel. The Seahorse XF Analyzer measured mitochondria respiration by detecting changes in oxygen (referred to as the oxygen consumption rate; OCR) following the addition of pharmacological agents: oligomycin, carbonyl cyanide m-chlorophenyl hydrazone (CCCP), rotenone and antimycin A. The functioning of mitochondria was determined as parameters expressed as % change max or basal OCR (depending on the functional readout). Spare capacity was measured as the difference between max and basal OCR. The average of five wells was taken for each sample per experimental replicate. Data presented as mean±SEM (n=15, 15, 7, 12 for groups PMCA, -80°C, PBSN and Untreat, respectively) and represent every experimental replicate performed. Statistical significance examined by Kruskal-Wallis test with a statistical criterion of 0.05. No statistical significance was found for all experimental comparisons